ICES Journal of Marine Science

ICES Journal of Marine Science (2016), 73(3), 897–909. doi:10.1093/icesjms/fsv194

Contribution to Special Issue: 'Towards a Broader Perspective on Ocean Acidification Research'

Original Article

Biochemical responses to ocean acidification contrast between tropical corals with high and low abundances at volcanic carbon dioxide seeps

J. Strahl[1]*, D. S. Francis[2], J. Doyle[1], C. Humphrey[1], and K. E. Fabricius[1]

[1]*Australian Institute of Marine Science, PMB 3, Townsville, MC, QLD 4810, Australia*
[2]*School of Life and Environmental Sciences, Centre for Chemistry and Biotechnology (Warrnambool Campus), Deakin University, Sherwood Park, PO Box 423, Warrnambool, VIC 3280, Australia*

**Corresponding author: tel: +61 7475 34312; fax +61 7475 35852; e-mail: j.strahl@aims.gov.au*

Strahl, J., Francis, D. S., Doyle, J., Humphrey, C., and Fabricius, K. E. Biochemical responses to ocean acidification contrast between tropical corals with high and low abundances at volcanic carbon dioxide seeps. – ICES Journal of Marine Science, 73: 897–909.

Received 27 April 2015; revised 29 September 2015; accepted 2 October 2015; advance access publication 2 November 2015.

At two natural volcanic seeps in Papua New Guinea, the partial pressure of carbon dioxide (pCO_2) in the seawater is consistent with projections for 2100. Here, the cover of massive scleractinian corals *Porites* spp. is twice as high at elevated compared with ambient pCO_2, while that of branching corals such as *Acropora millepora* is greater than twofold reduced. To assess the underlying mechanisms for such community shifts under long-term exposure to elevated pCO_2, biochemical parameters related to tissue biomass, energy storage, pigmentation, cell protection, and cell damage were compared between *Porites* spp. and *A. millepora* from control (mean $pH_{total} = 8.1$, $pCO_2 = 323$ μatm) and CO_2 seep sites (mean $pH_{total} = 7.8$, $pCO_2 = 803$ μatm) each at two reefs. In *Porites* spp., only one of the biochemical parameters investigated (the ratio of photoprotective to light-harvesting pigments) responded to pCO_2, while tissue biomass, total lipids, total proteins, and some pigments differed between the two reefs, possibly reflecting differences in food availability. Furthermore, some fatty acids showed pCO_2 – reef interactions. In *A. millepora*, most pigments investigated were reduced at elevated pCO_2, while other parameters (e.g. tissue biomass, total proteins, total lipids, protein carbonyls, some fatty acids and pigments) differed between reefs or showed pCO_2 – reef interactions. Tissue biomass, total lipids, and cell-protective capacities were distinctly higher in *Porites* spp. than in *A. millepora*, indicating higher resistance to environmental stress in massive *Porites*. However, our data suggest that important biochemical measures remain relatively unaffected in these two coral species in response to elevated pCO_2 up to 800 μatm, with most responses being smaller than differences between species and locations, and also when compared with responses to other environmental stressors such as ocean warming.

Keywords: energy storage, fatty acids, lipid classes, ocean acidification, oxidative stress, pigments, scleractinia, volcanic carbon dioxide seeps.

Introduction

Anthropogenic carbon dioxide (CO_2) emissions and rising partial pressures of carbon dioxide (pCO_2) in seawater are a major threat to highly productive and diverse coral reef ecosystems (Dove *et al.*, 2013). The oceans' uptake of atmospheric CO_2 leads to modifications of its seawater carbonate chemistry, including reductions in pH and carbonate ion concentration, in a process termed ocean acidification (OA). Most recently published literature shows that calcification decreases and decalcification processes increase in corals and coral reef ecosystems under OA (Erez *et al.*, 2011; Dove *et al.*, 2013).

At natural volcanic CO_2 seeps in Japan, Italy, and Papua New Guinea (PNG), pCO_2 conditions are consistent with projections for 2100 (RCP 6.0; IPCC, 2014). These seeps are unique places, where organisms are exposed to enhanced pCO_2 and changing seawater carbonate chemistry throughout their post-settlement life, while most experimental OA studies are short term (days–months, reviewed in Erez *et al.*, 2011). At the seeps, the densities of sensitive species and the diversity of benthic invertebrates are significantly reduced in the low compared with ambient pH zones (Fabricius *et al.*, 2011, 2014; Kroeker *et al.*, 2011). Consequently,

seep sites are dominated by generalists, robust enough to withstand acidified conditions (Kroeker *et al.*, 2011; Inoue *et al.*, 2013), such as massive scleractinian corals *Porites* spp. at the CO_2 seeps in PNG (Fabricius *et al.*, 2011; Strahl *et al.*, 2015).

Physiological studies conducted *in situ* at the seep sites may help to understand the processes that lead to the observed community shifts under high pCO_2. Two recent studies report that differences in the physiological responses of soft and hard coral species matched the observed differences in abundances at the high vs. ambient pCO_2 sites in Japan and PNG (Inoue *et al.*, 2013; Strahl *et al.*, 2015). The soft coral *Sarcophyton elegans*, which dominates medium pCO_2 zones of 830 μatm at the seeps in Japan, benefited from elevated pCO_2 (390–850 μatm) via enhanced photosynthesis, while net calcification remained stable (Inoue *et al.*, 2013). Similarly, at the Upa-Upasina seep site in PNG, dark and net calcification rates remained stable in the highly abundant massive *Porites* spp., but significantly declined in branching *Acropora millepora* and *Seriatopora hystrix* which both show considerably reduced abundances (−60 and −80%) at high compared with ambient pCO_2 (Strahl *et al.*, 2015).

To date, studies on the impact of OA on corals have focused mainly on calcification and photosynthesis (Erez *et al.*, 2011; Inoue *et al.*, 2013; Comeau *et al.*, 2014). They show that many species have declining calcification rates in response to high pCO_2, while other species show stimulation, hence estimates of changes in rates of calcification at twofold ambient atmospheric pCO_2 range from +23 to −78% (reviewed in Erez *et al.*, 2011). Similarly, rates and efficiency of photosynthesis can either increase or remain unaffected by pCO_2 (Schneider and Erez, 2006; Crawley *et al.*, 2010; Inoue *et al.*, 2013; Strahl *et al.*, 2015).

However, other physiological processes related to energy storage, cell protection, and cell damage are equally important as they influence organism health and indirectly affect biogenic calcium carbonate deposition (Pörtner, 2008; Kaniewska *et al.*, 2012). Assessing the effects of high pCO_2 on these processes may help to explain currently observed discrepancies in calcification and photosynthesis, and in the heterogeneity of responses and susceptibility of different coral species to OA. Two recent studies indicate that elevated pCO_2 may lead to higher levels of oxidative stress in corals and bivalves. In the coral *A. millepora*, genes involved in cellular antioxidant protection and in programmed cell death (apopotosis) were up-regulated after 28 d of exposure to 1010 μatm pCO_2 (Kaniewska *et al.*, 2012). Similarly, the oyster *Crassostrea virginica* up-regulated the expression of proteins associated with oxidative stress in response to >2000 μatm pCO_2 (e.g. superoxide dismutase, peroxiredoxins; Tomanek *et al.*, 2011). The mechanisms causing oxidative stress under hypercapnia and reduced oxygen conditions are not well understood, but for corals, it has been suggested that hypercapnia impairs the photosynthetic apparatus of the symbiotic *Symbiodinium* spp. and/or the mitochondria of the coral host tissue, leading to higher production rates of reactive oxygen species (Kaniewska *et al.*, 2012).

Oxidative stress can cause apoptosis, autophagy or necrosis, and the expulsion of photosynthetic *Symbiodinium* spp. from the coral host, a process called coral bleaching (Lesser, 2011). Richier *et al.* (2008) reported a loss of pigments and/or expulsion of *Symbiodinium* spp. as the first step of cellular defence against environmental stress (in this case, irradiance), while both chlorophyll *a* concentration and endosymbiont density declined in two coral species after 24 d of exposure to 600 μatm pCO_2 (Schoepf *et al.*, 2013). A loss of pigments and/or *Symbiodinium* spp. may lead to a decline in phototrophic energy generation in stressed corals, and subsequently, to depleted energy reserves such as lipids or proteins and/or to changing ratios of structural to storage lipids and changing fatty acid compositions (Bachok *et al.*, 2006; Imbs and Yakovleva, 2012). For example, lipid and fatty acid contents in corals declined 1.5- to 3-fold following bleaching events in Hawaii and Okinawa, while the proportion of structural lipids increased at the expenses of storage lipids (Grottoli *et al.*, 2004; Yamashiro *et al.*, 2005; Bachok *et al.*, 2006).

Energetic costs for corals may rise in the coming decades under projected pCO_2, e.g. due to an increasing need for active, ATP consuming ion regulation at the site of calcification (McCulloch *et al.*, 2012). In a recent study, an up-regulation of triglyceride lipase and Acyl-CoA dehydrogenase point to an increase in the breakdown of lipids for energy use in *A. millepora* under high pCO_2 (Kaniewska *et al.*, 2012). Conversely, energy reserves including lipids, proteins, and carbohydrates were largely maintained in four tropical and one Mediterranean hard coral species under a decreased pH of 7.8–7.9 (Bramanti *et al.*, 2013; Schoepf *et al.*, 2013).

The physiological effects of hypercapnia on cellular metabolic pathways in corals including energy storage, cellular protection, and production of reactive oxygen species are largely understudied and at present, data on corals exposed to high pCO_2 *in situ* (e.g. at volcanic CO_2 seeps) are lacking. A better understanding of these processes might explain the observed heterogeneity of responses and susceptibility/resilience of corals to OA, and might re-evaluate predictions of community shifts in tropical coral reefs in a future of projected pCO_2 (RCP 6.0; IPCC, 2014).

In the present study, two coral taxa were investigated after long-term exposure to OA at natural CO_2 seeps in PNG: (i) massive *Porites* spp., which have established dominance at the seep sites with a cover twice as high as under ambient pCO_2, and (ii) branching *A. millepora*, which are greater than twofold reduced at high pCO_2 (Fabricius *et al.*, 2011; Strahl *et al.*, 2015). Tissue biomass, contents of lipids and proteins, pigment concentrations, and oxidative stress parameters were compared in corals growing at two control and two CO_2 seep sites.

Material and methods

Site description and sampling of corals

The "seep" sites at Upa-Upasina Reef (S 9° 49.446′, E 150° 49.055′) and at Dobu Island (S 9° 44.199′, E 150° 52.060′) in Milne Bay Province, PNG, were near areas of CO_2 venting and had low pH and high pCO_2. Bubble streams consist of 99% CO_2 and 1% of O_2, N_2, and CH_4 (Fabricius *et al.*, 2011). The control sites with ambient pH and pCO_2 were located 0.5 and 2.5 km from the seep sites at Upa-Upasina Reef (S 9° 49.693′, E 150° 49.231′) and Dobu Island (S 9° 45.125′, E 150° 51.248′), respectively. Seawater samples were collected at the two control and two seep sites and analysed for temperature and carbonate chemistry parameters by Vogel *et al.* (2015). Water was repeatedly collected on several days in April/May 2012 and May/June 2013 incorporating diurnal fluctuations, with a total number of seawater samples of 36 (Vogel *et al.*, 2015). The seawater temperature was 29.5 ± 0.6°C. For Dobu and Upa-Upasina Reef, the pH_{Total} was 8.14 ± 0.03 (mean ± s.d.) at the control and 7.84 ± 0.11 at the seep sites. The concentration of dissolved inorganic carbon was 1914 ± 28 μmol kg^{-1} SW at the control and 2107 ± 52 μmol kg^{-1} SW at the seep sites. The pCO_2 and Ω_{AR} were 323 ± 31 μatm and 4.25 ± 0.32 at the control sites and 803 ± 252 μatm and 2.72 ± 0.54 at the seep sites (carbonate

chemistry data re-calculated from Vogel *et al.*, 2015, detailed description of all sites in Fabricius *et al.*, 2011).

Massive *Porites* spp. and *A. millepora* colonies were sampled by scuba diving in April 2012 from each of the two seep and two control sites at 4–5 m depth. For each species, six colonies were sampled that were >10 m apart, and duplicate samples were obtained from each colony (massive *Porites* spp.: fragments of 3–4 cm diameter, *A. millepora:* branchlets of ~4 cm length and 1 cm diameter). The samples were immediately snap-frozen in liquid nitrogen, and transported to the Australian Institute of Marine Science for biochemical analyses.

Sample preparation

To determine pigment content and tissue biomass, the two coral taxa had to be treated differently because the tissue of *Porites* spp. penetrates up to 5 mm deep into the tissue (Lough and Barnes, 1997) and is therefore not suitable for the air gun technique, while that of *A. millepora* is <1 mm thick. For *Porites* spp., one fragment per colony was crushed with a French press (Civilab, Australia), constantly cooled down with liquid nitrogen. Before crushing, the surface area of frozen *Porites* spp. was determined using the aluminium foil technique (Marsh, 1970). For *A. millepora,* the tissue was removed from the skeleton with an air gun in 10 ml of ultra-filtered (0.05 mm) seawater, and the coral homogenate was separated into host and *Symbiodinium* spp. fraction by centrifugation (3 min, 1500*g*, 4°C). Skeletons of *A. millepora* were dried overnight in the oven at 60°C and their surface area was determined using the single wax dipping technique (Veal *et al.*, 2010).

To determine all remaining biochemical parameters, the second fragment/branchlet of each *Porites* spp./*A. millepora* colony was crushed with a French press (Civilab, Australia), constantly cooled down with liquid nitrogen. Sixty per cent of this crushed material was freeze dried for 24 h (FD12 Freeze Dryer, Dynavac, USA) for determination of ash-free dry weight (AFDW), contents of total lipids, lipid classes, fatty acids, and total proteins. The remaining crushed material was stored at −80°C to analyse total antioxidant capacity (TAC) and protein carbonyls (i.e. proteins damaged by reactive oxygen species).

Biochemical investigations

Tissue biomass and total protein content

Protein content (host and *Symbiodinium* spp. fraction of first fragment/branchlet of each colony) per unit surface area was determined as an index of tissue biomass, while the total protein content (host and *Symbiodinium* spp. fraction of second fragment/branchlet) related to AFDW provided information on energy storage capacity. 0.1 g of freeze-dried crushed sample or 200 µl of coral homogenate was dissolved in 1 M NaOH 1:10 (w/v) or 1:1 (v/v) for protein quantification following Dove *et al.* (2006). The coral samples were homogenized, incubated for 1 h at 90°C and centrifuged for 10 min at 1500*g* and room temperature. The protein content of the supernatant (for determination of tissue biomass/total protein content) was determined spectrophotometrically (BioTek Powerwave microplate spectrophotometer, USA) using the DC protein assay kit (Bio-Rad Laboratories, Australia) with bovine serum albumin standards (Leuzinger *et al.*, 2003).

Total lipid content

Total lipid content was extracted from 1 to 2 g of freeze-dried sample in 4 ml of the solvent dichloromethane:methanol (CH_2Cl_2:CH_3OH) (2:1) according to Folch *et al.* (1957) and following the modifications of Conlan *et al.* (2014). The samples were sonicated (Ultrasonic processor XL heat systems, John Morris Scientific Pty, Australia) for 10 min and filtered into a scintillation vial. This process was repeated two times. The combined filtrates (~12 ml) were then washed with 6.5 ml of KCl (0.44%) in H_2O/CH_3OH (3:1). After 12 h incubation in the dark at room temperature, the bottom layer containing the extracted lipid was recovered and the solvent was evaporated under nitrogen. The lipid was then weighed and standardized to AFDW.

Tissue energy content (calories g^{-1} AFDW) was then calculated from enthalpies of combustion based on values by Gnaiger and Bitterlich (1984): lipid (39.5 kJ g^{-1}) and protein (23.9 kJ g^{-1}).

Lipid classes

A 250 µl subsample of the re-dissolved total lipid fraction was taken and analysed for lipid class composition using an Iatroscan MK 6 s thin layer chromatography—flame ionization detector (Mitsubishi Chemical Medience, Japan) according to Nichols *et al.* (2001) and following the modifications of Conlan *et al.* (2014). Briefly, each sample was spotted on silica gel S4-chromarods (5 µm particle size). Lipid separation followed a two-step elution sequence. First, elution of lyso-phosphatidylcholine (L-PC), phosphatidylcholine (PC), phosphatidylserine and phosphatidylinositol (PS-PI), and phosphatidylethanolamine (PE) was achieved in a dichloromethane:methanol:water (50:20:2, by volume) solvent. Second, elution of wax esters (WE), triacylglycerol (TG), free fatty acid (FFA) 1,3-diacylglycerol (1,3-DG), sterol (ST), and 1,2-diacylglycerol (1,2-DG) was achieved in a hexane:diethyl ether:formic acid (60:15:1.5, by volume) solvent. Individual lipid classes were collectively calculated as the ratio of storage (L-PC, PC, PS-PI, PE, ST) to structural (WE, TG, FFA, 1,3-DG, 1,2-DG) lipids.

Fatty acids

Fatty acids were esterified into methyl esters using the acid-catalyzed methylation method (Christie, 2003) following the protocol of Conlan *et al.* (2014). The purified hexane supernatant of the coral samples was placed in a gas chromatography (GC) vial for GC injection. Fatty acid methyl esters were isolated and identified using an Agilent Technologies 7890B GC System (Agilent Technologies, USA) equipped with a BPX70 capillary column (120 m × 0.25 mm internal diameter, 0.25 µm film thickness, SGE Analytical Science, Australia), a flame ionization detector (FID), an Agilent Technologies 7693 auto sampler, and a splitless injection system. The injection volumes, temperature sequences, and flow rates followed the protocol of Conlan *et al.* (2014). The carrier gas was hydrogen. The individual fatty acids were identified relative to known external standards (a series of mixed and individual standards from Sigma-Aldrich, Inc., St Louis, USA and Nu-Chek Prep Inc., USA), using the software GC ChemStation (Rev B.04.03, Agilent Technologies). The resulting peaks were corrected by theoretical relative FID response factors (Ackman, 2002) and quantified relative to the internal standard C23:0 (0.75 mg mg^{-1}, Sigma-Aldrich, Inc., USA).

Ash-free dry weight

Approximately 0.5 g of freeze dried and preweighed coral material was transferred into a preweighted aluminium container and burned for 5 h in the muffle furnace at 480°C. The AFDW of the sample was standardized to dry weight.

Total antioxidant capacity

TAC was measured with the OxiSelect™ Total Antioxidant Capacity Assay Kit (Cell Biolabs, USA) according to the

manufacturer's protocol. Samples of crushed corals were homogenized in phosphate-buffered saline (PBS, pH 7.4) at 1:3 (w/v), sonicated on ice for 40 s and centrifuged for 10 min at 10 000*g* and 4°C. Uric acid standards were prepared (0.0, 0.05, 0.1, 0.35, 0.6, and 1.0 mM) and 10 μl of the coral supernatant/standards was pipetted into wells of a 96-well microtitre plate. Initial and final absorbance

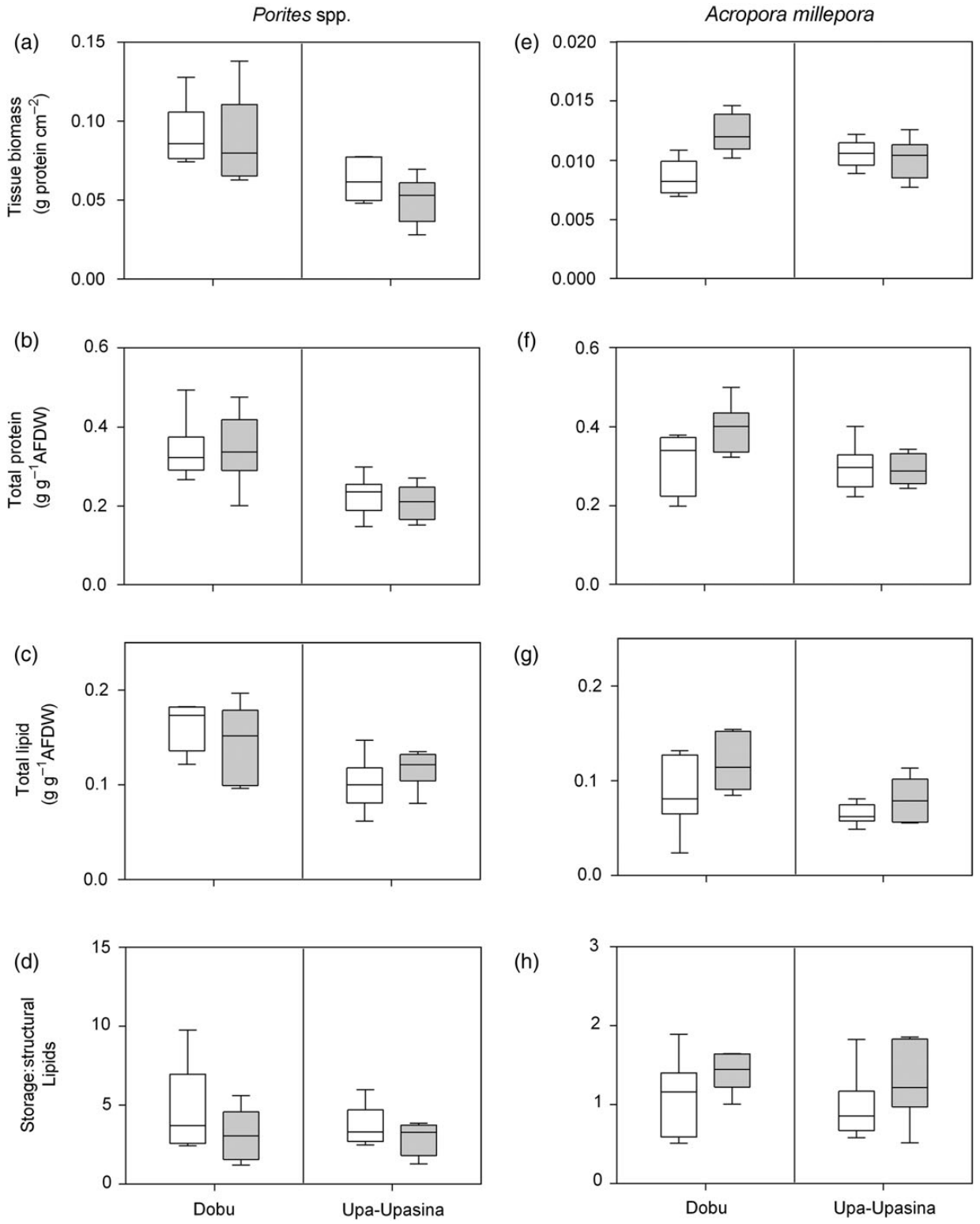

Figure 1. Tissue biomass (a and e) and contents of total protein (b and f) and lipid (c and g) and lipid classes (d and h) in massive *Porites* spp. and *A. millepora* at the control (ambient pCO_2, white boxes) and seep sites (high pCO_2, grey boxes) at the two reefs, $n = 6$ per species, reef/pCO_2 site, and parameter.

readings of samples/standards were conducted at 490 nm with the Synergy H4 microplate reader (BioTek, USA). The TAC was calculated in copper reducing equivalents standardized to the protein content of the sample.

Protein carbonyl content

The protein carbonyl content was assessed in corals by using an OxiSelect protein carbonyl enzyme-linked immunosorbent assay (ELISA) kit (Cell Biolabs, USA) according to the manufacturer's protocol. Briefly, crushed coral samples were resuspended in chilled 1× PBS (pH 7.4) at 1:13 (w/v) and homogenized in a Mini Beadbeater (Biospec Products, USA) for 2 min. The homogenate was then centrifuged for 10 min at 10 000*g* and 4°C, and the protein content of the supernatant was determined. The supernatant was diluted to 10 μg ml^{-1} protein in 1× PBS, and protein carbonyl-bovine serum albumin standards were prepared (0, 0.75, 3, 6 nmol protein carbonyl mg^{-1} protein). To a well of a 96-well protein binding plate, 100 μl of sample/standard was added and incubated overnight at 4°C. Subsequently, the wells were incubated for 45 min in 2,4-dinitrophenylhydrazine working solution and for 1 h in blocking solution. Immunodetection was performed using 2,4-dinitrophenol and horseradish peroxidase-conjugated antibodies provided by the manufacturer. Wells were incubated for 2 min in substrate solution before reading the absorbance at 450 nm with a Synergy H4 microplate reader (BioTek, USA). The protein carbonyl content of the samples was standardized to the protein content of the sample.

Symbiodinium spp. pigment content

Pigments from the complete *Symbiodinium* spp. pellet of *A. millepora* obtained during tissue stripping and from 0.5 g crushed fragment material of *Porites* spp. were sonicated and extracted on ice in the dark in two consecutive 1 h extractions in 2.5 ml of chilled (4°C) buffered methanol [98% MeOH/2% 0.5 M tetrabutylammonium acetate (TBAA) pH 6.5]. Filtered (0.2 μm) extracts were diluted 1:1 with 28 mM TBAA (pH 6.5), and injected into an ultra-performance liquid chromatography (UPLC) system (Acquity UPLC, Waters, USA). Injection volumes and flow rates, as well as gradient conditions and the reference pigments followed Uthicke *et al.* (2012). Pigment content of coral samples was quantified using calibration curves based on the run time and spectral signatures of reference pigments under the same running conditions, and related to surface area.

Statistical analysis

Statistical analyses were conducted with Graph Pad Prism (version 6, GraphPad Software, USA). Data were tested for normality (Kolmogorov–Smirnov test) and homogeneity of variances (Bartlett's test). Outliers of all datasets were identified and removed by ROUT outlier test. A two-way ANOVA was used to evaluate the effect of pCO_2 (ambient vs. high) and reef (Dobu vs. Upa-Upasina) on all physiological measures for each species. Tukey's HSD was used for *post hoc* examinations of significant interaction terms (pCO_2 × reef). Lipid class data were arcsine transformed and PP/LH and Dtx/(Dtx + Ddx) ratios were *log*-transformed before statistical analysis. The ratios of the mean values of the biochemical parameters in *Porites* spp. to *A. millepora* were *log*-transformed before testing the null hypothesis (=no species difference) with *t*-tests.

Results

Tissue biomass, total protein and lipid content, lipid classes, and fatty acids

In massive *Porites* spp., tissue biomass (protein content per unit surface area), total protein content (protein content related to AFDW), and total lipid content remained unaffected by pCO_2, but were higher (37, 36, and 29%) at Dobu compared with Upa-Upasina (Figure 1a–c, Table 1). Similarly, tissue energy content (=calculated from the total protein and lipid contents) was not affected by pCO_2, but was 33% higher at Dobu (3.38 ± 0.48 calories g^{-1} AFDW) than at Upa-Upasina (2.25 ± 0.35 calories g^{-1} AFDW, Table 1). The lipid classes were not significantly affected by pCO_2 or reef (Figure 1d). On average, the fractions of storage lipids were three times higher than structural lipids in *Porites* spp. (75 vs. 25% of total lipids). Saturated, polyunsaturated, and *n*-3 long-chain polyunsaturated fatty acids displayed a significant interaction between pCO_2 and reef (Tables 2 and 3). At ambient pCO_2, they were 42–51% higher at Dobu compared with Upa-Upasina (Tukey $p < 0.005$), whereas

Table 1. ANOVA results comparing biochemical parameters in *Porites* spp. and *A. millepora* at the control (ambient pCO_2) and seep site (high pCO_2) at Dobu and Upa-Upasina Reef.

	***Porites* spp.**			***Acropora millepora***		
	d.f.	***F***	***p*-value**	**d.f.**	***F***	***p*-value**
Tissue biomass						
pCO_2	1	1.112	0.305	1	7.185	**0.015**
Reef	1	15.100	**0.001**	1	0.021	0.887
pCO_2:reef	1	0.196	0.663	1	11.190	**0.003**
Residuals	19	–	–	19	–	–
Total protein						
pCO_2	1	0.061	0.808	1	2.651	0.119
Reef	1	18.160	**0.001**	1	5.535	**0.029**
pCO_2:reef	1	0.172	0.683	1	3.308	0.084
Residuals	19	–	–	20	–	–
Total lipid						
pCO_2	1	0.004	0.955	1	4.366	0.050
Reef	1	13.500	**0.002**	1	7.092	**0.015**
pCO_2:reef	1	1.911	0.182	1	0.572	0.459
Residuals	20	–	–	19	–	–
Tissue energy content						
pCO_2	1	0.065	0.802	1	9.046	**0.007**
Reef	1	39.510	**<0.001**	1	15.030	**0.001**
pCO_2:reef	1	0.246	0.626	1	5.601	**0.028**
Residuals	20	–	–	20	–	–
Storage:structural lipid						
pCO_2	1	2.432	0.135	1	3.191	0.090
Reef	1	0.700	0.413	1	0.013	0.911
pCO_2:reef	1	0.267	0.611	1	0.182	0.675
Residuals	20	–	–	20	–	–
Total antioxidant capacity						
pCO_2	1	0.122	0.731	1	0.228	0.639
Reef	1	0.041	0.842	1	0.243	0.627
pCO_2:reef	1	2.683	0.117	1	0.080	0.780
Residuals	20	–	–	20	–	–
Protein carbonyls						
pCO_2	1	0.498	0.489	1	0.288	0.598
Reef	1	0.097	0.759	1	5.193	0.034
pCO_2:reef	1	0.944	0.344	1	1.619	0.219
Residuals	19	–	–	19	–	–

Significant differences ($p < 0.05$) are highlighted in bold. d.f., degrees of freedom.

Table 2. Contents of fatty acids in mg g^{-1} AFDW in massive *Porites* spp. and *A. millepora* at the control (ambient pCO_2) and seep sites (high pCO_2) at the two reefs.

	Porites spp.				*Acropora millepora*			
	Dobu, control	Dobu, seep	Upa-Upasina, control	Upa-Upasina, seep	Dobu, control	Dobu, seep	Upa-Upasina, control	Upa-Upasina, seep
Saturates	66.6 ± 12.4	50.2 ± 13.1	37.3 ± 11.2	45.7 ± 8.0	29.9 ± 9.6	50.9 ± 21.4	36.1 ± 26.8	28.5 ± 14.0
Monounsaturates	15.7 ± 2.3	14.2 ± 3.9	8.8 ± 2.6	9.1 ± 2.2	3.0 ± 1.0	4.2 ± 1.6	2.4 ± 0.7	2.6 ± 0.9
Polyunsaturates	24.0 ± 2.6	21.6 ± 3.2	13.6 ± 2.6	16.8 ± 2.6	17.3 ± 6.1	21.7 ± 5.6	17.2 ± 8.8	15.2 ± 4.8
n-6 polyunsaturates	14.1 ± 1.7	13.0 ± 1.3	8.3 ± 2.1	10.0 ± 1.8	7.4 ± 2.6	9.9 ± 2.3	5.9 ± 2.1	6.5 ± 2.0
n-3 polyunsaturates	9.9 ± 1.7	8.7 ± 2.1	5.2 ± 1.7	6.8 ± 1.2	9.9 ± 3.9	11.8 ± 3.4	9.7 ± 4.6	8.7 ± 2.9
n-6 long chain	9.3 ± 1.3	9.4 ± 0.9	5.9 ± 1.7	6.6 ± 1.2	4.2 ± 1.7	4.7 ± 1.1	4.0 ± 1.6	3.9 ± 1.1
n-3 long chain	8.5 ± 0.6	6.5 ± 2.0	4.2 ± 1.7	5.1 ± 0.4	7.9 ± 3.1	9.5 ± 2.7	8.0 ± 3.8	7.0 ± 2.3

Displayed are means ± s.d., $n = 6$ per species and reef/pCO_2 site. *n*-6 long chain, *n*-6 long-chain polyunsaturated fatty acids; *n*-3 long chain, *n*-3 long-chain polyunsaturated fatty acids.

differences were not statistically significant between reefs at high pCO_2. Monounsaturated, *n*-6 polyunsaturated, *n*-3 polyunsaturated, and *n*-6 long-chain polyunsaturated fatty acids were significantly (32–40%) higher at Dobu compared with Upa-Upasina (Table 3).

In *A. millepora*, tissue biomass displayed a significant interaction between pCO_2 and reef. At Dobu, it was 44% higher at elevated compared with ambient pCO_2 (Tukey $p < 0.05$), whereas at Upa-Upasina, values were unaffected by pCO_2 (Figure 1e, Table 1). Total protein and lipid contents remained unaffected by pCO_2, but were significantly higher at Dobu compared with Upa-Upasina Reef (Figure 1f and g, Table 1). The tissue energy content displayed a significant interaction between pCO_2 and reef (Table 1). At Dobu, it was 28% higher at elevated (3.58 ± 0.59 calories g^{-1} AFDW) compared with ambient pCO_2 (2.56 ± 0.59 calories g^{-1} AFDW; Tukey $p < 0.005$), whereas at Upa-Upasina, values were unaffected by pCO_2 (2.34 ± 0.28 calories g^{-1} AFDW). Contents of lipid classes and fatty acids were not significantly affected by pCO_2 (Figure 1h, Tables 1–3). On average, the total lipid consisted 58% of storage and 42% of structural lipids. Monounsaturated and *n*-6 polyunsaturated fatty acids were 20–39% higher at Dobu compared with Upa-Upasina, while contents of all other fatty acids did not differ significantly between the two reefs (Tables 2 and 3).

TAC and protein carbonyls

In massive *Porites* spp., the TAC and the content of protein carbonyls were not affected by pCO_2 and reef (Figure 2a and b, Table 1).

In *A. millepora*, the TAC remained unaffected by pCO_2 and reef, while protein carbonyls were twice as high at Upa-Upasina compared with Dobu (Figure 2c and d, Table 1).

Symbiodinium spp. pigment content

In massive *Porites* spp., most *Symbiodinium* spp. pigment concentrations were not significantly affected by pCO_2 (Figure 3). However, the ratio of photo-protective (PP: Ddx, Dnx, diatoxanthin and β-carotene) to light harvesting (LH: chlorophyll *a*, chlorophyll *c2*, and peridinin) pigments increased significantly at elevated pCO_2 (Dobu: +8%, Upa-Upasina: +17%, Figure 3h, Table 4). Pigment concentrations significantly differed between the two reefs: chlorophyll *c2*, peridinin, and the combination of diadinoxanthin (Ddx) and dinoxanthin (Dnx) were 20–26% higher, and β-carotene concentrations were 56% lower at Dobu compared with Upa-Upasina, respectively (Table 4). Meanwhile, concentrations of chlorophyll *a*, diatoxanthin (Dtx), and the Dtx/(Dtx + Ddx) ratio (as an indicator of the xanthophyll cycle) were similar at all sites.

Table 3. ANOVA results comparing fatty acid groups in *Porites* spp. and *A. millepora* at the control (ambient pCO_2) and seep site (high pCO_2) at Dobu and Upa-Upasina Reef.

	Porites spp.			*Acropora millepora*		
	d.f.	*F*	*p*-value	d.f.	*F*	*p*-value
Saturates						
pCO_2	1	0.704	0.412	1	0.680	0.420
Reef	1	13.020	**0.002**	1	0.994	0.331
pCO_2:reef	1	6.956	**0.016**	1	3.110	0.094
Residuals	19	–	–	19	–	–
Monosaturates						
pCO_2	1	0.228	0.639	1	1.901	0.185
Reef	1	26.370	**<0.001**	1	5.219	**0.035**
pCO_2:reef	1	0.595	0.450	1	0.940	0.345
Residuals	19	–	–	18	–	–
Polyunsaturates						
pCO_2	1	0.103	0.752	1	1.488	0.238
Reef	1	35.150	**<0.001**	1	1.348	0.260
pCO_2:reef	1	4.708	**0.043**	1	0.197	0.663
Residuals	19	–	–	19	–	–
n-6 polyunsaturates						
pCO_2	1	0.146	0.707	1	2.584	0.125
Reef	1	35.530	**<0.001**	1	6.379	**0.021**
pCO_2:reef	1	3.691	0.070	1	0.934	0.347
Residuals	19	–	–	18	–	–
n-3 polyunsaturates						
pCO_2	1	0.035	0.854	1	0.083	0.776
Reef	1	21.110	**0.001**	1	1.130	0.301
pCO_2:reef	1	3.815	0.066	1	0.888	0.358
Residuals	19	–	–	19	–	–
n-6 long chain						
pCO_2	1	0.638	0.435	1	0.153	0.700
Reef	1	31.170	**<0.001**	1	0.727	0.404
pCO_2:reef	1	0.350	0.561	1	0.309	0.585
Residuals	19	–	–	19	–	–
n-3 long chain						
pCO_2	1	0.911	0.353	1	0.068	0.797
Reef	1	24.470	**0.001**	1	0.889	0.357
pCO_2:reef	1	5.942	0.026	1	1.003	0.329
Residuals	17	–	–	19	–	–

Significant differences ($p < 0.05$) are highlighted in bold; d.f., degrees of freedom. *n*-6 long chain, *n*-6 long-chain polyunsaturated fatty acids; *n*-3 long chain, *n*-3 long-chain polyunsaturated fatty acids.

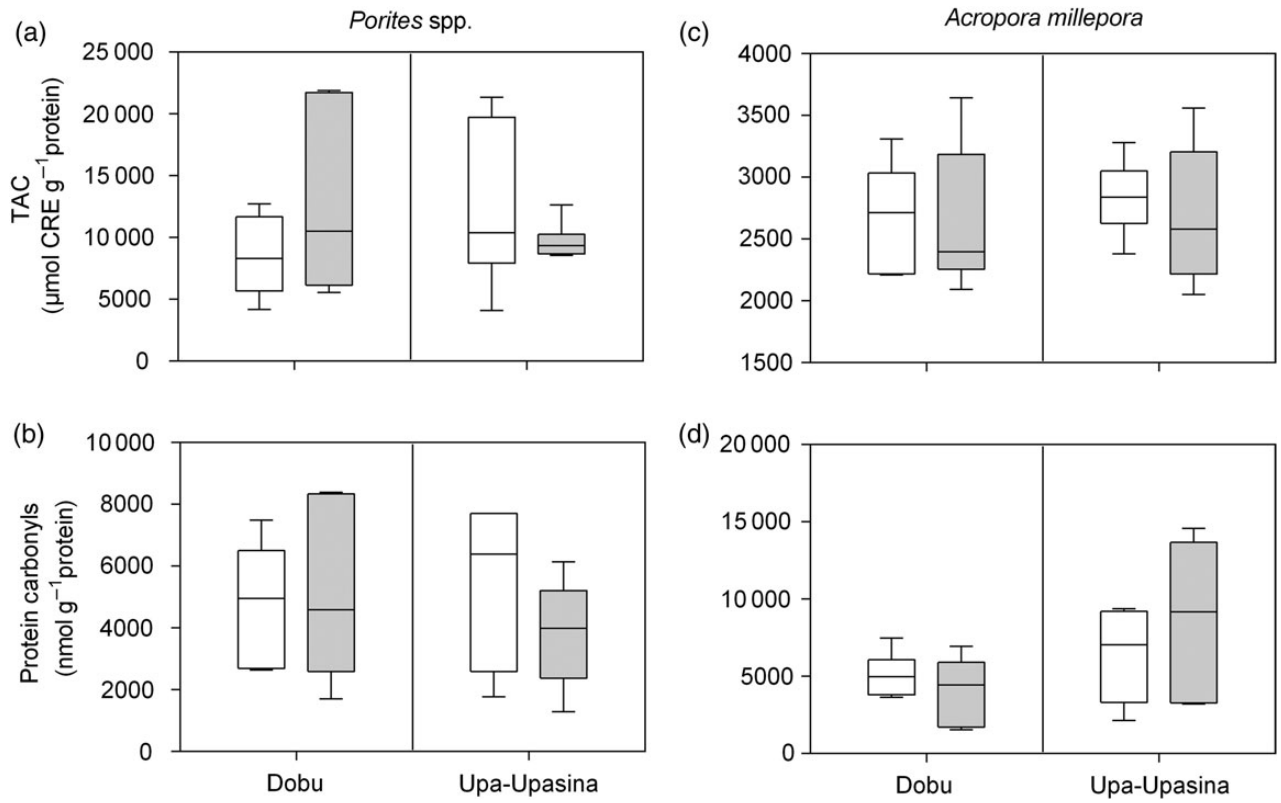

Figure 2. Total antioxidant capacity (TAC) (a and c) and content of protein carbonyls (b and d) in massive *Porites* spp. and *A. millepora* at the control (ambient pCO_2, white boxes) and seep sites (high pCO_2, grey boxes) at the two reefs, $n = 6$ per species, reef/pCO_2 site, and parameter.

In *A. millepora*, the concentrations of chlorophyll *a* and *c2*, peridinin, and the combination of Ddx and Dnx declined significantly by 22–31% at elevated pCO_2 at Dobu and Upa-Upasina (Figure 4a, c, and f), while β-carotene at elevated pCO_2 was reduced by 51% at Dobu and 88% at Upa-Upasina (Figure 4d, Table 4). Between sites, the concentrations of β-carotene and diatoxanthin were 73% and 31% lower at Upa-Upasina compared with Dobu (Figure 4d and e). Furthermore, the ratio of PP:LH and Dtx/(Dtx + Ddx) were 19% lower at Upa-Upasina compared with Dobu, respectively, while pCO_2 had no significant effect (Figure 4g and h, Table 4).

Comparison of massive *Porites* spp. and *A. millepora*

At ambient and elevated pCO_2, many of the energy-related and cell-protective parameters were significantly higher in *Porites* spp. than in *A. millepora* (Table 5). Tissue biomass was 5–11 times, total lipid content 1–2 times, TAC 3–5 times, and contents of LH and PP pigments 13–24 times higher in *Porites* spp. than in *A. millepora* at Dobu and Upa-Upasina Reef, while contents of total protein and protein carbonyls were similar in both corals (Table 5).

Discussion

We investigated *in situ* the effects of high pCO_2 on biochemical parameters in the apparently CO_2-resistant massive *Porites* spp., and the more CO_2-sensitive branching *A. millepora*. Our data support the conclusion of high tolerance of massive *Porites* spp. to elevated pCO_2. Tissue biomass, lipid, protein and tissue energy content, fatty acid content, pigment content, and oxidative stress parameters remained unaffected by pCO_2 up to ~800 µatm. Corals will experience such pCO_2 concentrations at the end of this century, should CO_2 emissions follow the representative concentration pathway 6.0 (IPCC, 2014). *Porites* spp. also shows unaltered net calcification rates after lifelong exposure to elevated pCO_2 at Upa-Upasina seeps (Fabricius *et al.*, 2011; Strahl *et al.*, 2015) and after experimental exposure to up to 1000 µatm pCO_2 for 2–4 weeks (Edmunds, 2011; Comeau *et al.*, 2014). In accordance, Edmunds (2011) reported that massive *Porites* maintained biomass and *Symbiodinium* spp. content at 400–800 µatm pCO_2, and McCulloch *et al.* (2012) identified *Porites* spp. as one of the most OA tolerant coral taxa due to their ability to maintain higher internal pH values at the site of calcification than many other species, as shown by boron isotope analysis. In contrast, *Acropora* spp. were classified as among the most sensitive coral species. Tissue biomass, total lipid content, and cell-protective capacities (e.g. TAC, photoprotective pigments) were much higher in *Porites* spp. compared with *A. millepora* at control and seep sites, which suggest increased resilience of the former to environmental stressors such as increased temperature or ultraviolet radiation.

Nevertheless, the physiological performance of *A. millepora* at the seep sites in PNG was unexpectedly strong, despite their greater than twofold lesser abundances and net calcification rates that were up to 50% reduced at the Upa-Upasina seep site in PNG (Fabricius *et al.*, 2011; Strahl *et al.*, 2015) and under experimentally increased pCO_2 (Schneider and Erez, 2006; Anthony *et al.*, 2008; Schoepf *et al.*, 2013). *Acropora millepora* was chosen for the study because, unlike for many other species of *Acropora*, enough colonies of this species existed at the seep sites to conduct the study. This may suggest that the CO_2 tolerance of this particular species may be higher than in other species of the genus *Acropora*. Most parameters investigated in *A. millepora* showed little negative responses to lifelong exposure to high pCO_2. Contents of protein and lipid as well as

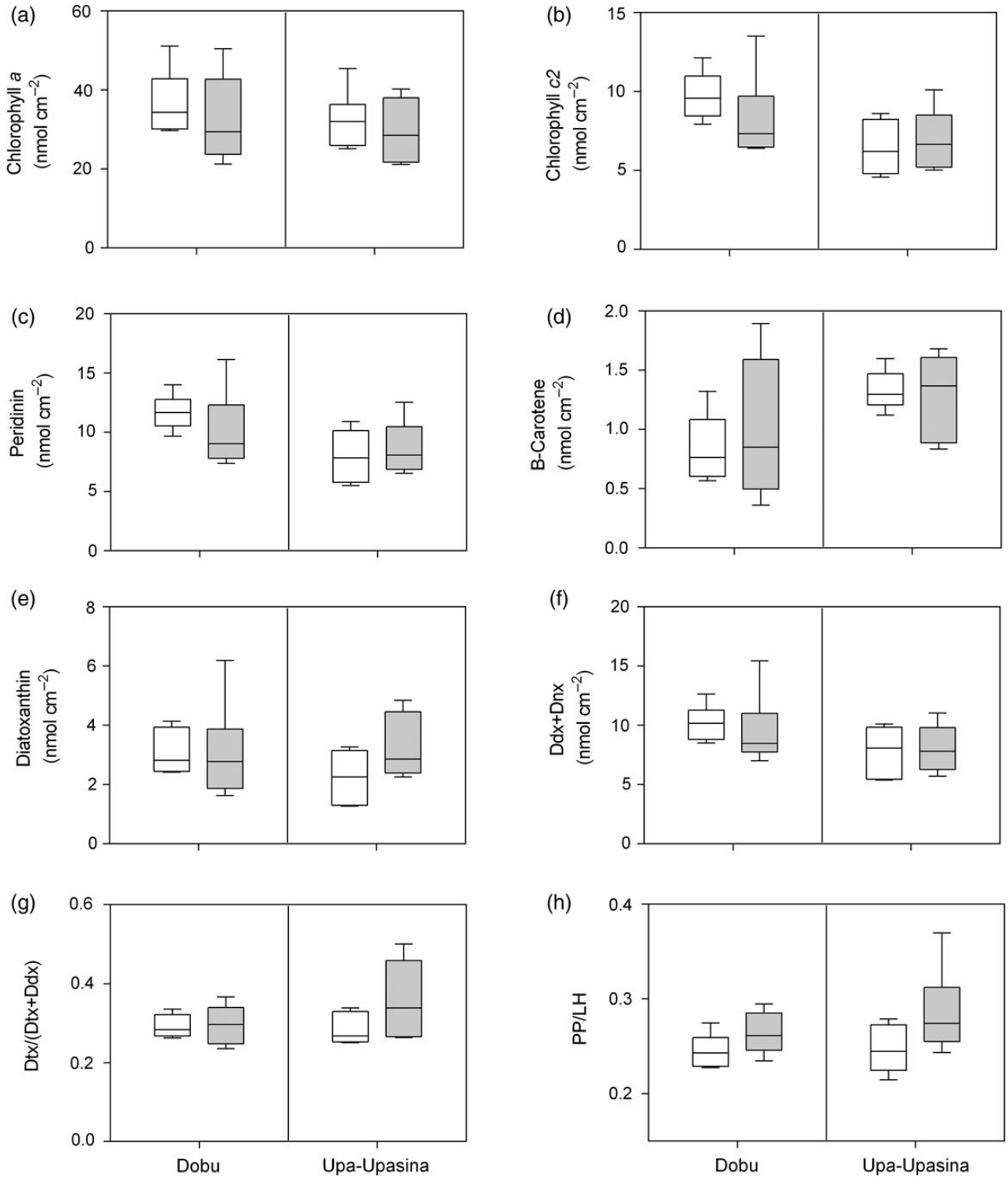

Figure 3. *Symbiodinium* spp. pigment content in massive *Porites* spp. at the control (ambient pCO_2, white boxes) and seep sites (high pCO_2, grey boxes) at the two reefs, $n = 6$ per reef/pCO_2 site and parameter. Dtx, diatoxanthin; Ddx, diadinoxanthin; Dnx, dinoxanthin; PP, photoprotective pigments; LH, light-harvesting pigments.

fatty acids, TAC, and protein carbonyls remained stable under acidified conditions, while tissue biomass and energy content at Dobu slightly increased at high pCO_2. A distinct pCO_2 impact was a significant reduction in many of the *Symbiodinium* spp. pigments in *A. millepora* at the seep sites.

Tissue biomass, proteins, and lipids

While calcification rates are traditionally investigated as a proxy of coral response to environmental stressors (reviewed in Erez *et al.*, 2011), biomass and energy reserves are often ignored as sensitive indicators for coral health. Corals with high biomass level and

Table 4. ANOVA results comparing pigment concentrations and pigment ratios in *Porites* spp. and *A. millepora* at the control (ambient pCO_2) and seep site (high pCO_2) at Dobu and Upa-Upasina reef.

	***Porites* spp.**			***Acropora millepora***		
	d.f.	***F***	***p*-value**	**d.f.**	***F***	***p*-value**
Chlorophyll *a*						
pCO_2	1	0.926	0.347	1	8.317	**0.009**
Reef	1	1.037	0.321	1	0.059	0.811
pCO_2:reef	1	0.036	0.851	1	0.130	0.722
Residuals	20	–	–	20	–	–
Chlorophyll *c2*						
pCO_2	1	0.362	0.554	1	6.964	**0.016**
Reef	1	8.042	**0.010**	1	0.096	0.760
pCO_2:reef	1	1.528	0.231	1	0.046	0.831
Residuals	20	–	–	20	–	–
Peridinin						
pCO_2	1	0.218	0.646	1	9.538	**0.006**
Reef	1	7.103	**0.015**	1	0.449	0.511
pCO_2:reef	1	1.418	0.248	1	0.011	0.919
Residuals	20	–	–	20	–	–
β-Carotene						
pCO_2	1	0.105	0.749	1	7.770	**0.012**
Reef	1	6.811	**0.017**	1	13.560	**0.002**
pCO_2:reef	1	1.273	0.273	1	0.442	0.514
Residuals	20	–	–	19	–	–
Diatoxanthin						
pCO_2	1	1.159	0.294	1	2.432	0.135
Reef	1	0.486	0.494	1	9.001	**0.007**
pCO_2:reef	1	1.229	0.281	1	0.294	0.594
Residuals	20	–	–	20	–	–
Ddx + Dnx						
pCO_2	1	0.073	0.790	1	7.769	**0.011**
Reef	1	4.559	**0.045**	1	1.408	0.249
pCO_2:reef	1	0.278	0.604	1	0.090	0.768
Residuals	20	–	–	20	–	–
Dtx/(Dtx + Ddx)						
pCO_2	1	2.666	0.118	1	0.045	0.835
Reef	1	1.275	0.272	1	7.755	**0.011**
pCO_2:reef	1	2.102	0.163	1	0.630	0.437
Residuals	20	–	–	20	–	–
PP/LH						
pCO_2	1	5.859	**0.025**	1	0.006	0.937
Reef	1	0.966	0.337	1	16.760	**0.001**
pCO_2:reef	1	0.704	0.411	1	0.010	0.923
Residuals	20	–	–	20	–	–

Significant differences ($p < 0.05$) are highlighted in bold. d.f., degrees of freedom; Dtx, diatoxanthin; Ddx, diadinoxanthin; Dnx, dinoxanthin; PP, photoprotective pigments (Ddx, Dnx, diatoxanthin, β-carotene); LH, light-harvesting pigments (chlorophyll *a* and *c2*, peridinin).

energy storages are more resilient and show higher rates of survival and recovery from bleaching than starved corals and corals with low biomass (Rodrigues and Grottoli, 2007; Thornhill *et al.*, 2011). This difference will become more critical with predicted increasing frequencies in bleaching events in the coming decades (Donner, 2009). On average, tissue biomass was 7-fold higher and lipid content 1.5-fold higher in massive *Porites* compared with *A. millepora* at the four sites in PNG, which will make the latter generally more susceptible to environmental stressors.

However, the reduced abundance of *A. millepora* at the seep compared with the control sites in PNG (Fabricius *et al.*, 2011; Strahl *et al.*, 2015) cannot be explained by these parameters. Tissue biomass, total protein and lipid content (as a proportion of AFDW), and tissue energy content in both *Porites* spp. and *A. millepora* were not impacted by high pCO_2. A coral that does not up-regulate energy expenditure towards skeletal growth under acidified conditions can instead maintain energy investment into tissue biomass. Strahl *et al.* (2015) showed that photosynthetic rates increased under elevated supply of CO_2 in *A. millepora* at the Upa-Upasina seep site, but both dark and net calcification significantly decreased (−117 and −44%; Strahl *et al.*, 2015), while soft-tissue-related parameters remained unaffected or increased (this study) at high pCO_2. Similarly, total lipid/protein content and tissue biomass were fully maintained or increased by 18–60% in *A. millepora* and *Stylophora pistillata* after exposure to enhanced pCO_2 (740 and >1900 μatm), while calcification rates decreased by 18–53% (Krief *et al.*, 2010; Schoepf *et al.*, 2013). The Mediterranean red octocoral *Corallium rubrum* responded to increased pCO_2 (800 μatm) for >10 months by decreasing calcification rates (−59%), while no changes were found in total lipid and protein content between control and acidified treatment (Bramanti *et al.*, 2013). In the present study, total carbohydrate content was not determined, but similar to total lipid and protein content, total carbohydrate content remained constant or increased in *A. millepora* and *C. rubrum* at experimentally elevated pCO_2s of 740–800 μatm (Bramanti *et al.*, 2013; Schoepf *et al.*, 2013).

In massive *Porites*, energy demands for tissue and skeletal growth seemed to be met at both high and low pCO_2. Neither tissue biomass, contents of total protein, lipid and tissue energy (this study), nor net calcification (Strahl *et al.*, 2015) showed any pCO_2 effect, but some of these measures contrasted between the reefs. Thus, despite the assumption that the energetic costs of calcification increase at high pCO_2 (Cohen *et al.*, 2009; Erez *et al.*, 2011), evidence is increasing that many species of scleractinian corals do not deplete their energy reserves to sustain calcification under acidified conditions (this study; Krief *et al.*, 2010; Bramanti *et al.*, 2013; Schoepf *et al.*, 2013). Instead, some species grow more slowly but maintain their energy reserves (e.g. *A. millepora*), possibly aided by higher photosynthetic carbon gain at elevated concentrations of dissolved inorganic carbon (this study; Strahl *et al.*, 2015). Further, high rates of heterotrophic feeding may prevent reductions in rates of calcification at high pCO_2 in some corals (Towle *et al.*, 2015). For example, the Caribbean coral *Acropora cervicornis* maintained growth rates at both elevated temperature and elevated CO_2 when fed, while unfed corals experienced significant decreases in growth (Towle *et al.*, 2015).

Lipid classes and fatty acids

The examination of lipid classes and fatty acids provides insights into how corals utilize their energy resources under different environmental conditions. Neither the lipid class composition nor total fatty acid content/proportions in *Porites* spp. and *A. millepora* were impacted by long-term exposure (up to 70 years, present study) to high pCO_2, which is in agreement with findings in *C. rubrum* after >10 months of exposure to enhanced pCO_2 (Bramanti *et al.*, 2013). In contrast, lower levels of key storage lipids, TG, and WE had been detected in *Porites* spp. and *Montipora verrucosa* after bleaching/warm-water events off the coasts of Hawaii and the Republic of Kiribati (Grottoli *et al.*, 2004; Carilli *et al.*, 2012). Similarly, both structural and storage lipids declined by 60–70% in stony corals (*Acropora intermedia, Montipora digitata*) and soft corals during a short-term heat stress experiment (33°C for 10–48 h; Imbs and Yakovleva, 2012). And after a heat stress and bleaching event in Japan in 2003, corals contained significantly lower total fatty acids as well as lower amounts of polyunsaturated fatty acids

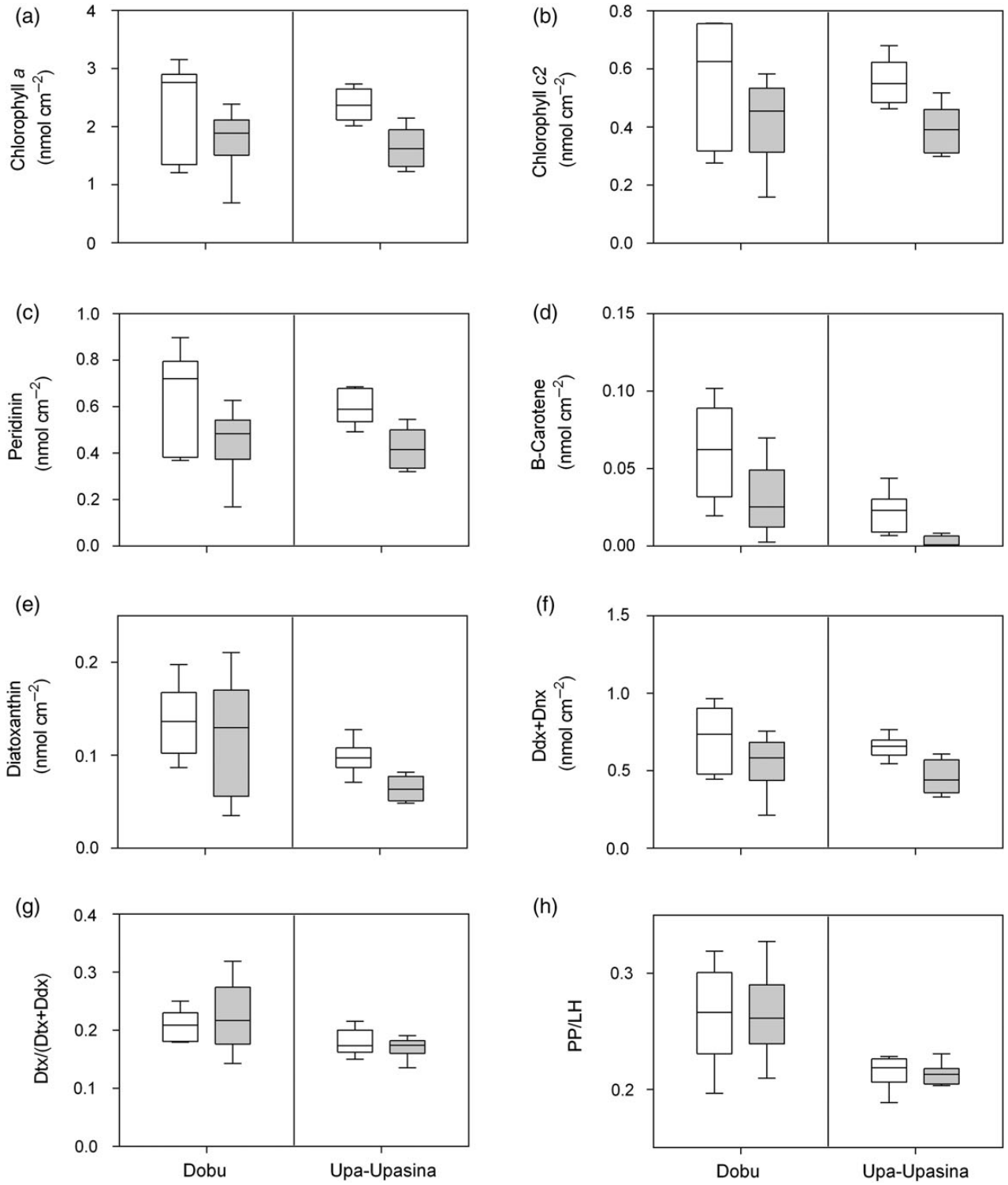

Figure 4. *Symbiodinium* spp. pigment content in *A. millepora* at the control (ambient pCO_2, white boxes) and seep sites (high pCO_2, grey boxes) at the two reefs, $n = 6$ per reef/pCO_2 site and parameter. Dtx, diatoxanthin; Ddx, diadinoxanthin; Dnx, dinoxanthin; PP, photoprotective pigments; LH, light-harvesting pigments.

and higher relative amounts of saturated and monounsaturated fatty acids (Bachok *et al.*, 2006). These studies and our data in combination suggest that increasing seawater temperatures and bleaching events are more stressful and energetically more costly for corals than elevated pCO_2 levels of up to 800 μatm.

Oxidative stress parameters

Total antioxidant capacities were on average 4-times higher, and photoprotective capacities 17-times higher in *Porites* spp. than in *A. millepora*, which will increase the resilience of massive *Porites* to increasing production rates of reactive oxygen species induced

Table 5. Ratios of the mean values of the biochemical parameters of *Porites* spp. to *A. millepora* at the control (ambient pCO_2) and seep sites (high pCO_2) at the two reefs, and their significance (*t*-test).

	Average, all sites	Dobu, control	Dobu, seep	Upa-Upasina, control	Upa-Upasina, seep	*t*-value	d.f.	*p*-value
Tissue biomass	7.2	10.7	7.0	6.0	5.0	11.69	3	**0.001**
Total protein content	0.9	1.1	0.9	0.8	0.7	1.54	3	0.222
Total lipid content	1.5	1.9	1.2	1.6	1.5	4.52	3	**0.020**
Light-harvesting pigments	18.5	15.6	19.3	15.1	24.0	26.81	3	**<0.001**
Photoprotective pigments	16.8	16.3	19.2	13.2	18.4	33.83	3	**<0.001**
Total antioxidant capacity	4.0	3.2	4.8	4.4	3.6	14.47	3	**<0.001**
Protein carbonyls	0.8	0.9	1.0	0.9	0.5	1.43	3	0.248

Tabled are ratios of tissue biomass (g protein cm^{-2}), total protein and lipid content (g g^{-1} AFDW), photoprotective and light-harvesting pigments (nmol cm^{-2}), total antioxidant capacity (μmol CRE g^{-1} protein), and protein carbonyls (nmol g^{-1} protein). Significant differences ($p < 0.05$) are highlighted in bold; d.f., degrees of freedom.

by environmental stressors (e.g. increasing seawater temperatures, solar ultraviolet radiation), which are known to directly induce photo-oxidative stress in corals (Lesser, 1996; Downs *et al.*, 2013).

However, oxidative stress parameters in massive *Porites* spp. and *A. millepora* were highly variable between colonies and were not considerably impacted by increased pCO_2. The activity of cellular protective antioxidants (e.g. TAC), which can be stimulated by enhanced production rates of harmful reactive oxygen species (Halliwell, 2006) in coral host tissues and photosynthetic active *Symbiodinium* spp., remained similarly high in corals at control and seep sites in the present study. In accordance, the contents of protein carbonyls remained unaffected by pCO_2 in both *Porites* spp. and *A. millepora*. Our findings do not support the hypothesis that mild hypercapnia might impair the photosynthetic apparatus of *Symbiodinium* spp. and/or the mitochondria of the coral host tissue, leading to higher production rates of reactive oxygen species (Kaniewska *et al.*, 2012).

Pigments

In the present study, light harvesting and photoprotective pigments decreased significantly (by 22–31% and 30–88%, respectively) in *A. millepora* at the seep compared with the control sites, but remained unaffected by pCO_2 in massive *Porites*. A decline of *Symbiodinium* spp./pigments in corals at high pCO_2 can be a sign of stress, indicating a breakdown in the symbiotic relationship due to changes in carbon concentrating mechanisms, photorespiration, and/or direct impacts of acidosis (Anthony *et al.*, 2008; Kaniewska *et al.*, 2012). Similar to our findings, Anthony *et al.* (2008) observed a stronger decline in pigmentation in *Acropora intermedia* (20% bleaching) than in *Porites lobata* (10% bleaching) exposed to pCO_2 and temperature conditions similar to the present study (pH 7.85 vs. 7.87, temperature 28–29°C vs. 29 °C). Muehllehner (2013) reported significantly reduced symbiont to host cell ratios in *A. millepora* (−54%) at the seep (~850 μatm pCO_2) compared with the control site of Upa-Upasina Reef *in situ* in August 2010, which supports the results of the present study. Similarly, the content of *Symbiodinium* spp. declined by 50% in *A. millepora* after 24–28 d of exposure to up to 1350 μatm pCO_2 (Kaniewska *et al.*, 2012; Schoepf *et al.*, 2013). Our pigment data support earlier studies stating that *Porites* spp. will be more resilient than *Acropora* spp. in a future of increasing pCO_2 (Fabricius *et al.*, 2011; McCulloch *et al.*, 2012; Comeau *et al.*, 2014; Strahl *et al.*, 2015).

Furthermore, the ratio of photoprotective to light-harvesting pigments (PP:LH) increased in massive *Porites* at the two seep sites, providing the coral with a higher level of photo protection as a response to the elevated photosynthetic activity. Strahl *et al.* (2015) reported a benefical effect of elevated pCO_2 on the photosynthetic rates in massive *Porites* (+43%) and *A. millepora* (24%) at Upa-Upasina Reef (corals at Dobu were not investigated in the study). The production rate of harmful reactive oxygen species potentially increases when rates of photosynthesis are high (Lesser, 1996). Photoprotective mechanisms in *Symbiodinium* spp. have been reported widely in the form of xanthophyll cycling and in their capacity to generate more photoprotective diatoxanthin pigments in response to environmental stressors (e.g. solar radiation; Ambarsari *et al.*, 1997; Brown *et al.*, 2002). Thus, an elevated ratio of PP:LH at high pCO_2 in *Porites* spp.—but not in *A. millepora*—will counteract oxidative damage accumulation and lead to a higher resistance of massive *Porites* to increasing reactive oxygen species concentrations.

Reef-related differences in biochemical parameters (Dobu vs. Upa-Upasina)

The observed differences in the physiological performance of corals between the two reefs may be related to potential differences in oceanographic conditions (e.g. currents, wave exposure, turbidity) and food availability, also demonstrating the difficulty to compare the effects of high pCO_2 between regions. Tissue biomass and contents of total lipid, protein, fatty acids, and pigments were significantly higher at Dobu compared with Upa-Upasina in *Porites* spp. and/or *A. millepora*, suggesting more effective heterotrophic feeding at Dobu. Similarly, photosynthesizing foraminifera species dominate Upa-Upasina sites, while heterotrophic species are more abundant at the Dobu sites (Uthicke *et al.*, 2013), which indicates a higher food supply/nutrient content at the latter reef. For example, concentrations of dissolved inorganic nutrients in seawater were twofold higher at the Dobu compared with Upa-Upasina sites in April 2012 and May 2013 (N. Vogel and S. Uthicke, pers. comm.), potentially fuelling organic enrichment of particulate matter at Dobu as one possible food source for corals. Previous studies report that some symbiotic corals show strong biochemical responses to heterotrophic feeding, e.g. lipid contents were two to fourfold higher in *A. millepora, Acropora valida*, and *Turbinaria mesenterina* at turbid, inshore reefs compared with offshore reefs (Anthony, 2006; Bay *et al.*, 2009). In accordance, fed *A. cervicornis* maintained ambient growth rates and showed highest lipid contents at elevated temperature and pCO_2 in an 8-week aquarium experiment, while unfed corals experienced significant decreases in growth and lipid content (Towle *et al.*, 2015). Well-fed corals also maintained photosynthetic efficiency and cell division rates of *Symbiodinium* spp. under temperature stress, while both parameters progressively declined in experimentally

starved corals (reviewed in Fabricius *et al.*, 2013). Thus, further investigation of corals in PNG under long-term OA (e.g. feeding experiments and measurements of photosynthesis, respiration, and calcification rates in corals at Dobu) and a more detailed biochemical and oceanographic characterization of ambient and high pCO_2 sites at Dobu and Upa-Upasina are required to more explicitly explain the observed reef-related differences in biochemical parameters.

Conclusion

Most of the biochemical parameters investigated in *Porites* spp. and *A. millepora* were less impacted than expected under lifelong exposure to predicted future pCO_2 (RCP6.0; IPCC, 2014) and can therefore not explain the observed community shift in coral reefs at the seep sites in PNG. Coral calcification more than other physiological parameters related to coral health (e.g. tissue biomass, energy storage capacity, cell damage) seem to be predominantly affected in pCO_2-sensitive corals such as *A. millepora* under lifelong exposure to high pCO_2 (this study; Strahl *et al.*, 2015). However, our study could not investigate any of the coral species most negatively affected by acidified conditions, because they were too rare at the seep sites to be included in this study. This suggests that the CO_2 tolerance of *A. millepora* may be higher than in those other species of the genus *Acropora* that were rare or absent at elevated pCO_2.

Our study and recent publications (Grottoli *et al.*, 2004; Carilli *et al.*, 2012; Imbs and Yakovleva, 2012) in combination show that other environmental stressors such as increasing seawater temperature and bleaching are energetically more costly for corals than OA alone. Key physiological and biochemical features in generalists such as massive *Porites* underpin their resilience to combined stressors (e.g. high pCO_2 and increasing sea surface temperature/bleaching) and support their recovery from stress events, while more sensitive coral species such as *A. millepora* have lower tolerance thresholds. This might lead to changes in species composition and reduced diversity in tropical coral reefs (Fabricius *et al.*, 2011; Inoue *et al.*, 2013; Strahl *et al.*, 2015) under projected pCO_2 and ocean warming. However, a better understanding of physiological mechanisms and responses in different coral taxa to OA, and especially to combined stressors such as lifelong increased pCO_2 and ocean warming is needed to predict the future of coral reef ecosystems.

Acknowledgements

We thank the communities at Upa-Upasina and Dobu for their permission to study the corals on their reef. Many thanks to S. Noonan, N. Vogel, S. Uthicke, and the crew of the M.V. Chertan for their support during the fieldwork, and to H. Martinez, S. Hinz, C. Assaille, K. Berry, and P. Buerger for their assistance in the laboratory. We thank P. Davern and M. Donaldson for their help with the logistics and shipment of the equipment, and QantasLink for continued support. This project was funded by the Australian Government's Super Science Initiative (Grant FS110200034), the Australian Government's National Environmental Research Programme, and the Australian Institute of Marine Science.

References

Ackman, R. G. 2002. The gas chromatograph in practical analyses of common and uncommon fatty acids for the 21st century. Analytica Chimica Acta, 465: 175–192.

Ambarsari, I., Brown, B. E., Barlow, R. G., Britton, G., and Cummings, D. 1997. Fluctuations in algal chlorophyll and carotenoid pigments during solar bleaching in the coral *Goniastrea aspera* at Phuket, Thailand. Marine Ecology Progress Series, 159: 303–307.

Anthony, K. R. N. 2006. Enhanced energy status of corals on coastal, high-turbidity reefs. Marine Ecology Progress Series, 319: 111–116.

Anthony, K. R. N., Kline, D. I., Diaz-Pulido, G., Dove, S., and Hoegh-Guldberg, O. 2008. Ocean acidification causes bleaching and productivity loss in coral reef builders. Proceedings of the National Academy of Sciences of the United States of America, 105: 17442–17446.

Bachok, Z., Mfilinge, P., and Tsuchiya, M. 2006. Characterization of fatty acid composition in healthy and bleached corals from Okinawa, Japan. Coral Reefs, 25: 545–554.

Bay, L., Ulstrup, K. E., Nielsen, H. B., Jarmer, H., Goffard, N., Willis, B. L., Miller, D. J., *et al.* 2009. Microarray analysis reveals transcriptional plasticity in the reef building coral *Acropora millepora*. Molecular Ecology, 18: 3062–3075.

Bramanti, L., Movilla, J., Guron, M., Calvo, E., Gori, A., Dominguez-Carrió, C., Grinyó, A., *et al.* 2013. Detrimental effects of ocean acidification on the economically important Mediterranean red coral (*Corallium rubrum*). Global Change Biology, 19: 1897–1908.

Brown, B., Dunne, R., Goodson, M., and Douglas, A. 2002. Experience shapes the susceptibility of a reef coral to bleaching. Coral Reefs, 21: 119–126.

Carilli, J., Donner, S. D., and Hartmann, A. C. 2012. Historical temperature variability affects coral response to heat stress. PloS ONE, 7: e34418.

Christie, W. W. 2003. Lipid Analysis, Isolation, Separation, Identification and Structural Analysis of Lipids, 3rd edn. The Oily Press, Bridgewater, UK.

Cohen, A. L., McCorkle, D. C., de Putron, S., Gaetani, G. A., and Rose, K. A. 2009. Morphological and compositional changes in the skeletons of new coral recruits reared in acidified seawater: insights into the biomineralization response to ocean acidification. Geochemistry, Geophysics, Geosystems, 10: Q07005.

Comeau, S., Carpenter, R. C., Nojiri, Y., Putnam, H. M., Sakai, K., and Edmunds, P. J. 2014. Pacific-wide contrast highlights resistance of reef calcifiers to ocean acidification. Proceedings of the Royal Society of London Series B: Biological Science, 281: 20141339.

Conlan, J. A., Jones, P. L., Turchini, G. M., Hall, M. R., and Francis, D. S. 2014. Changes in the nutritional composition of captive early-mid stage *Panulirus ornatus* phyllosoma over ecdysis and larval development. Aquaculture, 434: 159–170.

Crawley, A., Kline, D., Dunn, S., Anthony, K. R. N., and Dove, S. 2010. The effect of ocean acidification on symbiont photorespiration and productivity in *Acropora formosa*. Global Change Biology, 16: 851–863.

Donner, S. D. 2009. Coping with commitment: projected thermal stress on coral reefs under different future scenarios. PloS ONE, 4: e5712.

Dove, S., Klinea, D. I., Pantosa, O., Anglyd, F. E., Tysond, G. W., and Hoegh-Guldberga, O. 2013. Future reef decalcification under a business-as-usual CO_2 emission scenario. Proceedings of the National Academy of Science of the United States of America, 110: 15342–15347.

Dove, S., Ortiz, J. C., Enriquez, S., Fine, M., Fisher, P., Iglesias-Prieto, R., Thornhill, D., *et al.* 2006. Response of holosymbiont pigments from the scleractinian coral *Montopora monasteriata* to short-term heat stress. Limnology and Oceanography, 51: 1149–1158.

Downs, C. A., McDougall, K. E., Woodley, C. M., Fauth, J. E., Richmond, R. H., Kushmaro, A., Gibb, S. W., *et al.* 2013. Heat-stress and light-stress induce different cellular pathologies in the symbiotic dinoflagellate during coral bleaching. PloS ONE, 8: e77173.

Edmunds, P. J. 2011. Zooplanktivory ameliorates the effects of ocean acidification on the reef coral *Porites* spp. Limnology and Oceanography, 56: 2402–2410.

Erez, J., Reynaud, S., Silverman, J., Schneider, K., and Allemand, D. 2011. Coral calcification under ocean acidification and global change. *In* Coral Reefs: an Ecosystem in Transition, pp. 151–176. Ed. by S. Dubinsky, and N. Stambler. Springer, New York.

Fabricius, K. E., Cséke, S., Humphrey, C., and De'ath, G. 2013. Does trophic status enhance or reduce the thermal tolerance of scleractinian corals? A review, experiment and conceptual framework. PloS ONE, 8: e54399.

Fabricius, K. E., De'ath, G., Noonan, S., and Uthicke, S. 2014. Ecological effects of ocean acidification and habitat complexity on reef-associated macroinvertebrate communities. Proceedings of the Royal Society of London Series B: Biological Science, 281: 20132479.

Fabricius, K. E., Langdon, C., Uthicke, S., Humphrey, C., Noonan, S., De'ath, G., Okazaki, R., *et al.* 2011. Losers and winners in coral reefs acclimatized to elevated carbon dioxide concentrations. Nature Climate Change, 1: 165–169.

Folch, J. M., Less, M., and Sloane-Stanley, G. H. 1957. A simple method for the isolation and purification of total lipides from animal tissues. The Journal of Biological Chemistry, 226: 497–509.

Gnaiger, E., and Bitterlich, G. 1984. Proximate biochemical composition and caloric content calculated from elemental CHN analysis: a stoichiometric concept. Oecologia, 62: 289–298.

Grottoli, A. G., Rodrigues, L. J., and Juarez, C. 2004. Lipids and stable carbon isotopes in two species of Hawaiian corals, *Porites compressa* and *Montipora verrucosa*, following a bleaching event. Marine Biology, 145: 621–631.

Halliwell, B. 2006. Reactive species and antioxidants. Redox biology is a fundamental theme of aerobic life. Plant Physiology, 141: 312–322.

Imbs, A. B., and Yakovleva, I. M. 2012. Dynamics of lipid and fatty acid composition of shallow-water corals under thermal stress: an experimental approach. Coral Reefs, 2012: 41–53.

Inoue, S., Kayanne, H., Yamamoto, S., and Kurihara, H. 2013. Spatial community shift from hard to soft corals in acidified water. Nature Climate Change, 3: 683–687.

IPCC. 2014. Climate Change 2014: impacts, adaptation, and vulnerability. *In* Contribution of Working Group II to the Fifth Assessment Report of the Intergovernmental Panel on Climate Change. Ed. by C. B. Field, V. R. Barros, D. J. Dokken, K. J. Mach, M. D. Mastrandrea, T. E. Bilir, M. Chatterjee, *et al.* Cambridge University Press, Cambridge, UK and New York, NY, USA.

Kaniewska, P., Campbell, P. R., Kline, D. I., Rodriguez-Lanetty, M., Miller, D. J., Dove, S., and Hoegh-Guldberg, O. 2012. Major cellular and physiological impacts of ocean acidification on a reef building coral. PloS ONE, 7: e34659.

Krief, S., Hendy, E. J., Fine, M., Yamd, R., Meibom, A., Foster, G. L., and Shemesh, A. 2010. Physiological and isotopic responses of scleractinian corals to ocean acidification. Geochimica and Cosmochima Acta, 74: 4988–5001.

Kroeker, K. J., Michelia, F., Gambib, M. C., and Martz, T. R. 2011. Divergent ecosystem responses within a benthic marine community to ocean acidification. Proceedings of the National Academy of Science of the United States of America, 108: 14515–14520.

Lesser, M. P. 1996. Elevated temperatures and ultraviolet radiation cause oxidative stress and inhibit photosynthesis in symbiotic dinoflagellates. Limnology and Oceanography, 41: 271–283.

Lesser, M. P. 2011. Coral bleaching: causes and mechanisms. *In* Coral Reefs: an Ecosystem in Transition, pp. 405–419. Ed. by S. Dubinsky, and N. Stambler. Springer, New York.

Leuzinger, S., Anthony, K. R. N., and Willis, B. L. 2003. Reproductive energy investment in corals: scaling with module size. Oecologia, 136: 524–531.

Lough, J. M., and Barnes, D. J. 1997. Several centuries of variation in skeletal extension, density and calcification in massive *Porites* colonies from the Great Barrier Reef: a proxy for seawater temperature and a background of variability against which to identify unnatural change. Journal of Experimental Marine Biology and Ecology, 211: 29–67.

Marsh, J. A. 1970. Primary productivity of reef-building calcareous red algae. Ecology, 51: 255–263.

McCulloch, M., Falter, J., Trotter, J., and Montagna, P. 2012. Coral resilience to ocean acidification and global warming through pH up-regulation. Nature Climate Change, 2: 623–627.

Muehllehner, N. 2013. The relationship between carbonate chemistry and calcification on the Florida Reef Tract, and in the symbiotic reef coral, *Acropora cervicornis*. Dissertation, University of Miami. http://scholarlyrepository.miami.edu/oa_dissertations.

Nichols, P. D., Mooney, B. D., and Elliot, N. 2001. Unusually high levels of non-saponifiable lipids in the fishes escolar and rudderfish: identification by gas and thin-layer chromatography. Journal of Chromatography A, 936: 183–191.

Pörtner, H.-O. 2008. Ecosystem effects of ocean acidification in times of ocean warming: a physiologist's view. Marine Ecology Progress Series, 373: 203–217.

Richier, S., Cottalorda, J. M., Guillaume, M. M., Fernandez, C., Allemand, D., and Furla, P. 2008. Depth-dependant response to light of the reef building coral, *Pocillopora verrucosa*: Implication of oxidative stress. Journal of Marine Biology and Ecology, 357: 48–56.

Rodrigues, L. J., and Grottoli, A. G. 2007. Energy reserves and metabolism as indicators of coral recovery from bleaching. Limnology and Oceanography, 52: 1874–1882.

Schneider, K., and Erez, J. 2006. The effect of carbonate chemistry on calcification and photosynthesis in the hermatypic coral *Acropora eurystoma*. Limnology and Oceanography, 51: 1284–1293.

Schoepf, V., Grottoli, A. G., Warner, M. E., Cai, W-J., Melman, T. F., Hoadley, K. D., Pettay, D. T., *et al.* 2013. Coral energy reserves and calcification in a high-CO_2 world at two temperatures. PloS ONE, 8: 1–11.

Strahl, J., Stolz, I., Uthicke, S., Vogel, N., Noonan, S., and Fabricius, K. E. 2015. Physiological and ecological performance differs in four coral taxa at a volcanic carbon dioxide seep. Comparative Biochemistry and Physiology, Part A, 184: 179–186.

Thornhill, D. J., Rotjan, R. D., Todd, B. D., Chilcoat, G. C., Iglesias-Prieto, R., Kemp, D. W., LaJeunesse, T. C., *et al.* 2011. A connection between colony biomass and death in Caribbean reef-building corals. PloS ONE, 6: e29535.

Tomanek, L., Zuzow, M. J., Ivanina, A. V., Beniash, E., and Sokolova, I. M. 2011. Proteomic response to elevated pCO_2 level in eastern oysters, *Crassostrea virginica*: evidence for oxidative stress. The Journal of Biology, 214: 1836–1844.

Towle, E. K., Enochs, I. C., and Langdon, C. 2015. Threatened Caribbean coral is able to mitigate the adverse effects of ocean acidification on calcification by increasing feeding rate. PloS ONE, 10: e0123394.

Uthicke, S., Momigliano, P., and Fabricius, K. E. 2013. High risk of extinction of benthic foraminifera in this century due to ocean acidification. Scientific Reports, 3: 1769–1774.

Uthicke, S., Vogel, N., Doyle, J., Schmidt, C., and Humphrey, C. 2012. Interactive effects of climate change and eutrophication on the dinoflagellate-bearing benthic foraminifera *Marginopora vertebralis*. Coral Reefs, 31: 401–414.

Veal, C. J., Carmi, M., Fine, M., and Hoegh-Goudberg, O. 2010. Increasing the accuracy of surface area estimation using single wax dipping of coral fragments. Coral Reefs, 29: 893–897.

Vogel, N., Fabricius, K. E., Strahl, J., Noonan, S. H. C., Wild, C., and Uthicke, S. 2015. Calcareous green alga *Halimeda* tolerates ocean acidification conditions at tropical carbon dioxide seeps. Limnology and Oceanography, 60: 263–275.

Yamashiro, H., Oku, H., and Onaga, K. 2005. Effect of bleaching on lipid content and composition of Okinawan corals. Fisheries Science, 71: 448–453.

Handling editor: Howard Browman